Journal of Macromolecular Science, Part A
Publication details, including instructions for authors and subscription information:
http://www.informaworld.com/smpp/title~content=t713597274

Characterization of Hydrocarbon Soluble Metal Oxides. Precursors to Supported Catalysts

Edwin A. Lewis[a]; Mohammed Habib[a]; Charles U. Pittman Jr.[a]
[a] Department of Chemistry, University of Alabama University, Alabama

To cite this Article Lewis, Edwin A. , Habib, Mohammed and Pittman Jr., Charles U.(1981) 'Characterization of Hydrocarbon Soluble Metal Oxides. Precursors to Supported Catalysts', Journal of Macromolecular Science, Part A, 15: 5, 915 — 939
To link to this Article: DOI: 10.1080/00222338108056776
URL: http://dx.doi.org/10.1080/00222338108056776

J. MACROMOL. SCI.-CHEM., A15(5), pp. 915-939 (1981)

Characterization of Hydrocarbon Soluble Metal Oxides. Precursors to Supported Catalysts

Edwin A. Lewis , Mohammed Habib, and Charles U. Pittman, Jr.

Department of Chemistry
University of Alabama
University, Alabama 35486

ABSTRACT

The metal oxide carboxylate complexes described in the previous chapter have been characterized by infrared spectroscopy, x-ray diffraction, electron microscopy, and analytical ultracentrifugation. The molecular weights and solution particle diameters have been determined for a number of the hydrocarbon soluble particles by analytical ultracentrifugation methods, and the use of a spherical model consistent with the particulate shape observed by electron microscopy. The size of the soluble complexes has been studied as a function of: metal, metal/acid ratio, acid composition, and solvent. The molecular weights for the ultimate particles are reasonably independent of the metal employed in the synthesis and are relatively constant for materials with similar metal/acid equivalents ratios. The single particle molecular weights for the complexes studied ranged from approximately 5×10^4 to 1.5×10^6 g mole^{-1}. The solution size distribution was polydisperse in all cases, with aggregates of the ultimate particles prevalent. Weight average molecular weights in excess of 10^9 g mole^{-1} have been observed. The aggregation is dependent on the surface acid composition and on the solvent in which the soluble complex is dispersed. Solubility and stability of these materials have been examined in a number of solvents. The metal oxide particles are initially soluble in octane, iso-octane, cyclohexane, mineral spirits, carbon tetrachloride, benzene, and tetrahydrofuran. However, most of the complexes eventually precipitate from dilute solutions in carbon tetrachloride,

benzene, and tetrahydrofuran. The stability of the particles is decreased in the presence of oxygen, or when carboxylic acids, alcohols, or ketones are present even in small amounts, and is decreased even further at temperatures above 100°C. Heterogeneous catalysts have been prepared by deposition of several of the soluble metal oxides onto supports such as alumina, silica, or kieselguhr followed by oxidation to yield supported metal oxides or reduction to yield supported metal. The application of few supported metals and metal oxides in hydrogenations of olefins, benzene, and naphthalene is described.

INTRODUCTION

In the preceding chapter entitled "Homogenizing Metal Oxide Catalysts" we described the synthesis and some potential applications of a new type of high molecular weight soluble metal oxide carboxylate complex. Any catalytic activity of the soluble metal oxide particles must depend to a large degree on the availability of the metallic core region to the reactants in solution, and therefore both the surface to volume ratio and the surface structure in terms of carboxylate coating density must be extremely important. A schematic diagram of the particulate structure is presented in Figure 1. In looking at this structure it should be obvious that an

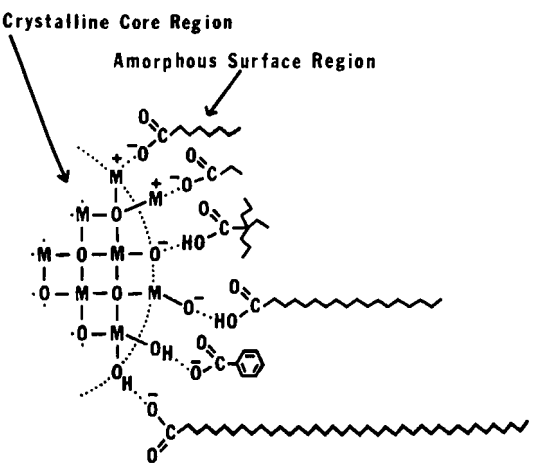

Figure 1. Schematic drawing of the crystalline core region of a metal-carboxylate complex.

increase in particle diameter would place a smaller fraction of the metal ions at the core surface, but it is more difficult to draw any conclusions about the dependence of reagent accessibility of the core on particle size. Nevertheless, one of the more important characteristics of these materials must be their molecular size, with the largest complexes expected to more closely resemble heterogeneous catalysts while the smallest complexes should look more like homogeneous catalysts. A very attractive feature of these oil soluble metal oxide particles is that the conditions of synthesis and the composition of the complex can apparently be manipulated to produce particles with a range of sizes. This ability to control the solution size of catalytically active particles could lead to the tailoring of the catalytic properties of these materials to specific applications. In addition the variation in solution size could presumably be exploited in the preparation of the supported metal and metal oxide catalysts, for example in controlling the catalytic site density or supported metal cluster size distribution.

The initial tasks of the work presented here were to elucidate the chemical structure of the novel hydrocarbon soluble metal oxide carboxylates and to determine the factors that influence size and solubility of the particles. In this regard the choice of metal, the metal/acid equivalents ratio, and the acid composition have been examined as synthesis variables, while solvent, polar solvent additives, oxidizing and reducing conditions, and temperature have been examined as post synthetic variables affecting size, solubility and structural stability. The final task of these investigations was to explore the application of the hydrocarbon-soluble metal oxides to the preparation of supported metal and metal oxide catalysts. In this regard supported metal and metal oxide materials were prepared from their hydrocarbon soluble complexes and tested in hydrogenation reactions.

EXPERIMENTAL

Preparation of Hydrocarbon Soluble Metal Oxides. The detailed synthesis of the soluble metal oxide particles has been described

in detail by Alkaitis and Cells in their 1979 patent (1), and was schematically diagrammed in the previous chapter (see figure 1, previous chapter). The synthesis of one specific complex of CoO is described below and some of the metals, carboxylic acids, and metal/acid equivalents ratios that have been utilized in the preparation of other complexes are listed in Table 1. It should be pointed out, that not all possible combinations implied in Table 1 have been prepared or examined; however, the information in this table does serve to indicate the range of variation possible in the complex preparation. The synthesis can be accomplished from either the metal or metal oxide and a mixture of two or more acids (usually three) mixed in the desired equivalents ratio.

The specific procedure for preparation of a cobalt carboxylate material is as follows. A mixture of 3 parts of propionic acid, 23 parts of neodecanoic acid, 49 parts C_{9-13} acid (neo-isomers), 2 parts polypropylene glycol, 0.2 parts of an antioxidant, 32 parts of mineral spirits, 12 parts cobalt metal, and 5 parts water was charged to a reaction vessel. The mixture was agitated and heated

Table 1

Metal Oxide Carboxylate Complex Component Variations.[a]

Metal or Metal Oxide Employed:	Cr, Mn, Fe, Co, Ni, Cu, Mn-Co			
Carboxylic Acids Employed:	C_3, C_8, neo C_{10}, C_{18}, C_{40}, Benzoic			
Typical Acid	15% C_3 23% C_8 62% neo C_{10}	20% C_3 70% neo C_{10} 10% C_{18}	20% C_3, 50% C_8 15% neo C_{10} 15% C_{18}	25% C_3, 20% C_8 25% C_{10}, 15% C_{18} 15% C_{40}
Metal/Acid Equivalents Ratio:	6, 12, 18, 24, 30, 36, 42			

a. All possible variations have not been prepared or investigated.

b. Several acid mixtures not listed here have been employed including many with aromatic acid moieties comprising from 5 to 15% of the mixture.

to 75°C. Air was then purged through the batch as an oxygen source to promote the reaction. Upon completion of the reaction the material was heated in the absence of air to 150°C to remove water. The product was cooled, filtered, and diluted with mineral spirits. The resulting soluble CoO carboxylate had a metal/acid equivalents ratio of approximately 6.0.

Structural Studies. Infrared studies were done on CCl_4 and hydrocarbon solutions, and on films of the hydrocarbon soluble metal oxide samples dried on salt plates. The infrared spectra of the complexes were compared to reference spectra for carboxylic acids and carboxylate salts, with particular attention to a comparison of the bands arising from both monomeric and dimerized carboxylic acid groups.

X-ray diffraction experiments were done on CCl_4 and hydrocarbon solutions of the metal oxide complexes. Diffraction patterns were obtained using a powder type camera with the liquid samples held in a glass capillary, which was noncrystalline and highly transparent to x-rays. The crystal phase identification was made in reference to the diffraction patterns of known materials.

Transmission electron microscopy studies of samples prepared by evaporation of CCl_4 solutions on Formvar film were made along with electron diffraction studies. The micrographs were normally taken at 2,000,000 x magnification and the diffraction patterns were recorded with a sample to photographic plate distance of 50 cm. The crystalline phase identification was again made in reference to the electron diffraction patterns of known materials.

Solution Molecular Weight and Particle Size Measurements. The metal oxide particle size and molecular weight in solution was examined by the use of sedimentation velocity techniques employing an analytical ultracentrifuge. These experiments were the method of choice since colligative property measurements would severely underestimate the complex size as the metal oxide particle solutions contain significant amounts of dissociated carboxylic acid and

perhaps even small amounts of simple metal ion carboxylates, and because gel permeation chromatography experiments would also suffer from such association equilibria and from the expected interactions between the gel matrix and the particulate surfaces. Initial attempts to determine particle molecular weights by sedimentation equilibrium methods also failed, as particle aggregation occurring during the time required to reach an equilibrium concentration distribution in the centrifuge cell resulted in precipitation of aggregates rather than achieving a distribution of the ultimate particles. This aggregation process has been examined further and will be discussed later in this chapter. Subsequent sedimentation equilibrium measurements on a few samples in good solvents have corraborated the velocity results.

All of the ultracentrifuge measurements were done using a Beckman Model E analytical ultracentrifuge equipped with a photoelectric scanner. All experiments employed an AnD rotor run at speeds of from 5,000 to 20,000 rpm and the temperature was controlled at 20°C. The cells employed double sector aluminum centerpieces with Kel-F gaskets and the scanner was operated in the split beam absorbance mode. Sample solutions had absorbances of approximately 0.5 in the wavelength range of 280 to 450 nm. The sedimentation coefficients, S, were calculated from the least squares slope of the logarithim of the boundary radius plotted as a function of time. The partial specific volumes, $\bar{v}$, for the soluble complexes were calculated from the densities of concentrated solutions of known composition. In all cases the $\bar{v}$ values were close to the weighted average of the reciprocal of the metal oxide and carboxylic acid densities, thus the assumption of limited (i.e. negliglble) preferential solvation appeared to be a reasonable one.

The use of sedimentation velocity data along with a spherical model for the solution complex shape has allowed the determination of molecular weights and particle diameters by combination of the following equations:

$$S = \frac{M(1-v\rho)}{Nf} \quad (1)$$

$$f = 6\pi\eta R_s \quad (2)$$

$$R_s = \frac{3\bar{v}M}{4\pi N}\ 1/3 \quad (3)$$

where S is the sedimentation coefficient, M is the molecular weight, $\bar{v}$ is the partial specific volume, ρ is the solution density, N is Avogadros number, f is the fricitional coefficient for a sphere, η is the solvent viscosity, and R_s is the spherical particle radius. The use of a spherical model seemed to be a reasonable assumption and electron micrographs have shown both the ultimate particles and the aggregates to be spherical when solvent is evaporated to leave a particulate film.

Supported Catalysts Prepared from Soluble Metal Oxides. The preceeding chapter described the deposition of several soluble metal oxide preparations onto supports such as alumina, Silica, or Kieselguhr followed by oxidation with oxygen, to give supported metal exides, and reduction with hydrogen or other reagents ($AlEt_3$ or $NaBH_4$), to give supported metals. The preparation of several other supported heterogeneous catalysts from the soluble metal oxides is now described.

Scheme I, A. shows the preparation of an alumina-supported cobalt oxide and cobalt from soluble cobalt oxide particles (Co/acid = 42). These catalysts were employed in olefin, benzene, and naphthalene hydrogenations. Two types of Kieselguhr-supported nickel catalysts were prepared as shown in Scheme I, B. The first was reduced with hydrogen and the second with $AlEt_3$. These were used in the hydrogenation of benzene. An alumina supported iron and an alumina-supported mixed cobalt iron catalysts were prepared as shown in Scheme I,C. and Scheme I,D. respectively. These catalysts were also tested in the hydrogenation of benzene.

Scheme I.

A. Alumina Supported CoO and Co.

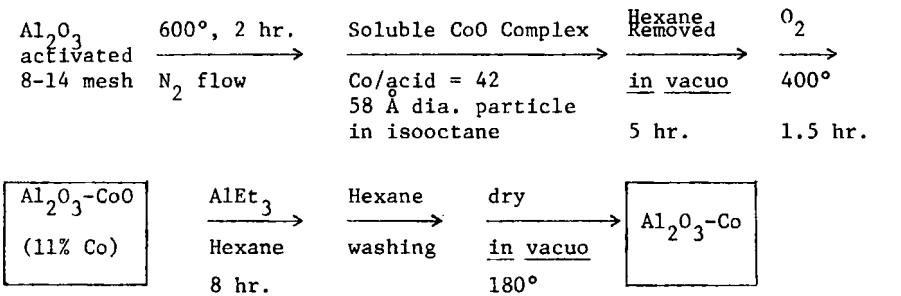

B. Kieselguhr Supported Ni.

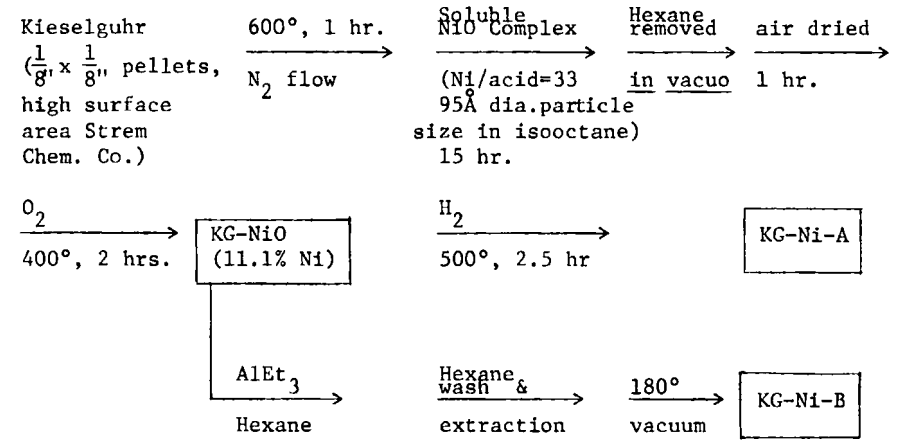

RESULTS AND DISCUSSION

Soluble Metal Oxide Carboxylate Structure. The formation of a metal carboxylate salt is characterized in the IR by the formation of a strong asymmetric vibrational band in the region from 1650-1540 cm^{-1} and a somewhat weaker symmetric stretch at 1450-1360 cm^{-1}. The former replaces the corresponding acid C=O band at 1740-1680

C. Alumina Supported Fe.

Al_2O Activated 8-14 mesh Fisher —200°, 2 hr. in vacuo→ Soluble Fe_2O_3 Complex Fe/acid = 9 5 hr. —pentane removed in vacuo→ —air dried 1 hr.→

—O_2 500°, 2 hr.→ [Al_2O_3-Fe_2O_3 10% Fe] —$AlEt_3$/hexane 12 hrs., 25°→

—Hexane wash→ —180°, 2 hr. in vacuo→ [Al_2O_3-Fe]

D. Alumina Supported Co/Fe.

Al_2O_3 activated 8-14 mesh Fisher —200° in vacuo→ Mixture of Soluble CoO and Fe_2O_3 Complexes 3 hr. —pentane removed in vacuo→ —air dried 1 hr.→

—200°, 1 hr. in vacuo→ —O_2 500°, 2 hr.→ [Al_2O_3-CoO-Fe_2O_3 5% Co, 5% Fe]

—$AlEt_3$ (Hexane) 25°→ 1) washed with Hexane → [Al_2O_3-Co-Fe]
2) 180°, 2 hr. in vacuo

cm^{-1} and the characteristic acid dimer band at 960-875 cm^{-1} disappears. The spectra of all of the soluble metal oxide carboxylates are indicative of carboxylate salts, RCO_2M.

In addition to indicating the type of acid-metal bonding, the infrared spectra in the region of 3600-3000 cm^{-1} reveal a

characteristic difference in the -OH absorption between the high molecular weight soluble metal oxides and simple metal carboxylate soaps. The presence of extensive hydrogen bonding of the -OH is evident in the spectra of the soluble complexes while only minor if any -OH and H-bonding is observed for the soaps. The large amount of -OH and H-bonding seen in the complexes is logically associated with the inorganic or metal portion of the particle. The infrared studies are consistent with the particulate structure shown in Figure 1 and would seem to corraborate the hypothesis of core (inorganic) and surface (carboxylate salt) regions.

When solutions of the soluble metal oxides were subjected to FeK radiation both crystalline and amorphous scattering patterns were observed. The sharpness of the lines in the diffraction patterns obtained on these solutions was indicative of crystallites in the 100-300 Å size range. The diffraction from the crystalline phase was sufficiently distinctive that the crystalline domains could be identified by reference to the diffraction patterns of known metal oxides. Crystallites of Mn_3O_4, CoO, Fe_3O_4, and CuO were observed in complex particulate solutions while the amorphous scattering was attributed to the metal carboxylate surface region surrounding the metal oxide crystalline core region. Of course the amorphous patterns were not sufficiently distinctive for phase identification, however, the mere demonstration of crystalline regions is sufficient to distinguish between low metal/acid equivalents ratio complexes (soaps) and the high metal/acid equivalents ratio materials we were investigating. Again the X-ray diffraction results are in accord with the structural model given in Figure 1.

Electron microscopy and electron diffraction studies on dried samples of the soluble metal oxide complexes demonstrated the particulate nature of these materials and corraborated the x-ray identification of the crystalline core regions of the complexes. Figure 2 shows a typical electron micrograph for a complex preparation. The material shown here is a Mn_3O_4 complex (Mn/acid = 18) and the ultimate particle size, about 3 mm on the print, corresponds

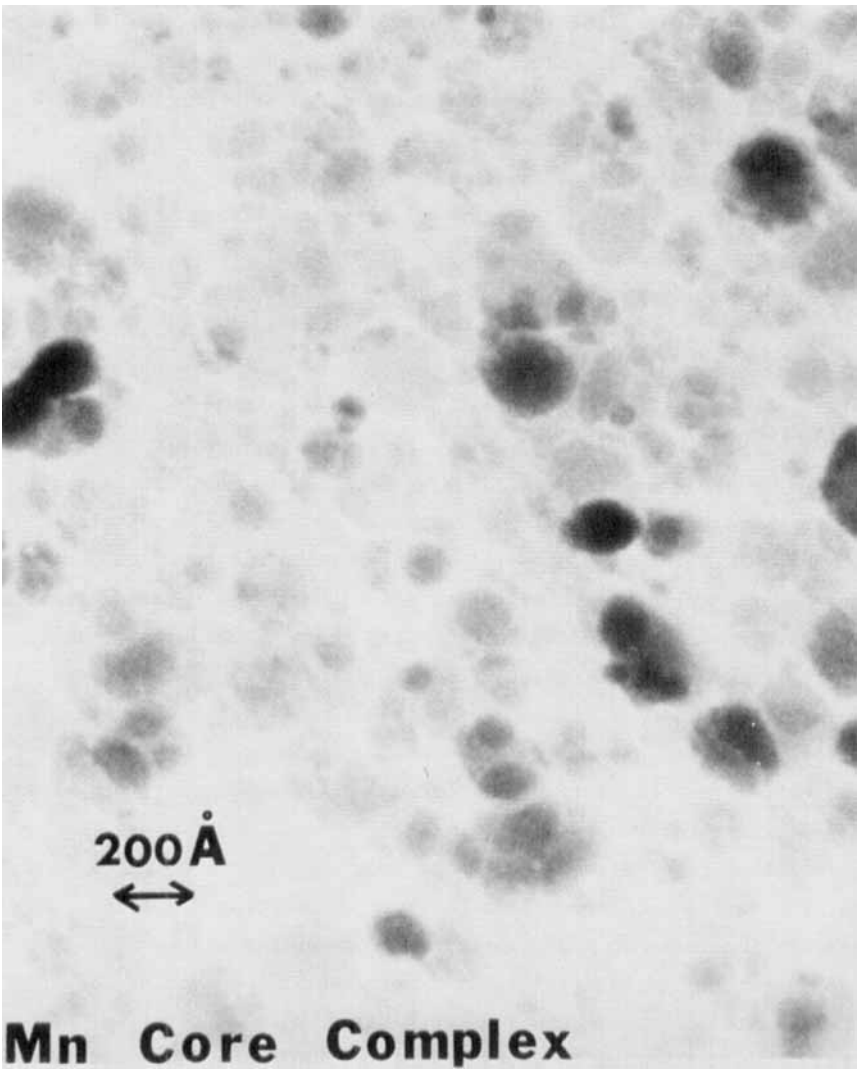

Figure 2. Electron micrograph of a carbontetrachloride evaporated sample of a soluble Mn_3O_4 complex with a metal/acid ratio of 18.

to a diameter of approximately 50 Å. In addition to the ultimate particles, larger particles, 200 to 300 Å in diameter and appearing to be aggregates of the smaller units, are prevalent. Both the solution particle size distribution and the aggregation of particles in solution as opposed to the dried film particulate dimensions will be discussed below. It should also be obvious from examination of Figure 2 that both the ultimate particles and aggregates are well described as spheres. Again the electron microscopy studies substantiate the hypothetical structure we presented in Figure 1.

Solution Size, Size Distrubution, and Controlling Factors. In the preceding chapter we presented three conclusions about the soluble metal oxide solution size; 1) the ultimate particle size tended to increase as the metal/acid equivalents ratio increased, 2) the particule size was independent of surface acid composition in a good solvent, and 3) particle aggregation was quite solvent dependent. Actually the situation is even somewhat more complicated.

The very first sedimentation experiments we conducted gave an indication that the soluble metal oxide particles were present in a distribution of sizes. Even for a single sample the size distribution was apparently dependent on the solvent and to a lesser degree on variations in the sedimentation velocity experiment itself, e.g. rotor speed.

The solution size measurements were complicated to an extreme degree by both surface equilibria and ultimate particle aggregation, even in good solvents. These complications foiled completely our early attempts at determining the molecular weight distributions by sedimentation equilibrium methods. We then decided to get estimates of the particle's solution diameters from the sedimentation coefficients measured in sedimentation velocity experiments combined with the use of a spherical model to calculate the frictional coefficients. The particle solution dimensions obtained from the sedimentation velocity measurements were in

excellent agreement with the size estimates made from the electron micrographs of dried solutions. In addition all of the hydrodynamic experiments corraborated the complex model given in Figure 1.

Figure 3 illustrates three different types of sedimenting boundaries that were observed in various ultracentrifuge experiments on the soluble metal oxides. Single sharp boundaries were only rarely seen, while both single broad boundaries (indicative of polydisperse samples) and multiple boundaries (indicative of mixtures of discrete particles) were quite commonly observed. We have labeled samples exhibiting broad boundaries as containing non-specific aggregates of ultimate particles while solutions showing multiple boundaries are labeled as containing specific aggregates. These two aggregation models are shown schematically in Figure 4. The type of aggregation a particular soluble complex participates in must be determined by the particulate surface topography (dependent on acid distribution and solvent) and by packing considerations.

Prior to continuing our discussion of the aggregation equilibria and the concommittant solubility effects we would like

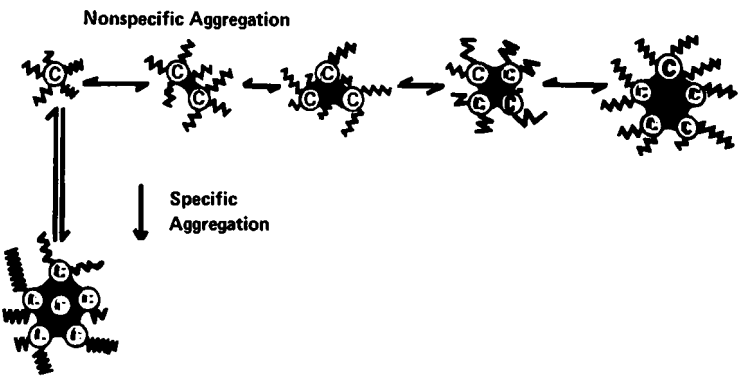

Figure 3. Schematic drawing of nonspecific and specific aggregation models. The nonspecific case yields a continuum of particle sizes while the specific yields only discrete particle sizes.

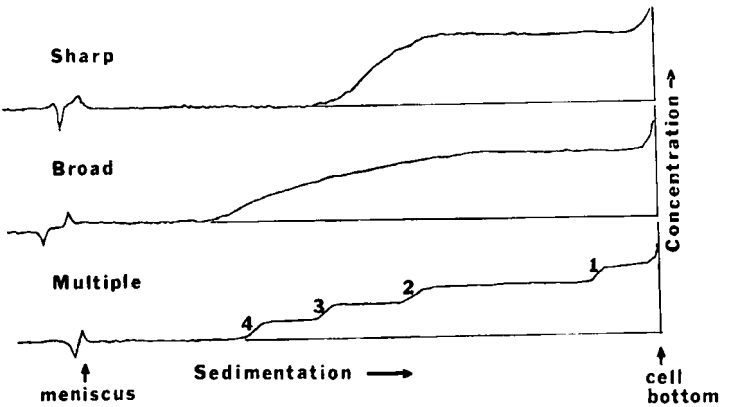

Figure 4. Boundary morphology as traced from the photoelectric scanner recordings of three different velocity experiments

to briefly review the solution size effects described in the previous chapter. Tables 2 and 3 summarize representative sedimentation velocity work and report the molecular weights and particle diameters for a number of complex metal oxide carboxylates in various solvents. Table 2 presents the data on a number of different Mu_3O_4 core complexes, while Table 3 presents the data on CoO, NiO, CuO, and mixed CoO/Mu_3O_4 complexes. The particle sizes in these tables are for the ultimate particle where multiple boundaries were observed but are for average particles where single broad boundaries were present.

The first three entries in Table 2 are for Mn_3O_4 cores with the same composition for the surface acid groups. These data illustrate that as the metal/acid equivalents ratio is increased; and all other factors are held constant, the molecular weight and the particle diameter increase. This would be the expected result with fewer acids complexing the metal oxide and larger metal oxide crystalline domains prevailing. It seems obvious that at some point the solubility of the particle surface would no longer be sufficient to allow dispersion of the particle, but this limit is difficult to determine experimentally. In the cases observed in this study

Table 2

Selected Hydrodynamic Data for Soluble Manganese Oxide Carboxylates

Metal	M/A (equivalent ratio)	Sedimentation coefficient(s)	Molecular Weight	Diameter	Solvent
Mn (Mn_3O_4)	6[a]	29	$6.3X10^4$	35	Mineral Spirits
Mn (Mn_3O_4)	12[a]	38	$1.2X10^5$	43	"
Mn (Mn_3O_4)	18[a]	52	$1.5X10^5$	48	"
	18[b]	51	$1.5X10^5$	47	"
	18[c]	49	$1.4X10^5$	47	"
	18[d]	52	$1.5X10^5$	48	"
Mn (Mn_3O_4)	18[d]	104	$0.5X10^6$	72	Cyclohexane
		184	$1.2X10^6$	80	Octane
		214	$1.2X10^6$	95	Isooctane
		220	$1.5X10^6$	103	CCl_4
		281	$1.9X10^6$	111	Benzene
		369	$2.9X10^6$	128	THF

[a]Acid composition 25% C_3, 25% C_8, 25% C_{10}, 15% C_{18}, and 10% benzoic acid

[b]Acid composition 35% C_3, 35% C_8, 10% C_{10}, 15% C_{18}, and 5% benzoic acid

[c]Acid composition 50% C_4, 40% C_8, 10% C_{18}

[d]Acid composition 40% C_4, 40% C_8, 20% C_{18}

it appears that the solubility is decreased mainly by particle aggregation, and that the maximum ultimate particle has not been observed for any of the metal/acid ratios achieved so far. Entries three through six in Table 2 illustrate the apparent independence of particle size on acid composition, while entries seven through twelve show an apparent dependence on solution particle size on the solvent in which the metal oxide carboxylates are dispersed. The increase in particle size in CCl_4, benzene, and THF is thought to be due to the aggregation of the ultimate particles by one of the schemes illustrated in Figure 4. The hypothesis is that

Table 3

Selected Hydrodynamic Data for Soluble Metal Oxide Carboxylates.

Metal	M/A (equivalent ratio)	Molecular Weight	Diameter A	Solvent
Co(CoO)	24[a]	$8.9X10^5$	86	Isooctane
		$4.6X10^6$	148	Benzene
		$5.7X10^6$	160	CCl_4
		$7.4X10^6$	180	Min. Spirits
Co(CoO)	42[a]	$5.3X10^5$	74	Isooctane
		$8.9X10^6$	180	Benzene
		$1.1X10^7$	206	Min. Spirits
		$3.3X10^9$	1270	CCl_4
Ni(NiO)	33[b]	$9.0X10^5$	90	Isooctane
		$3.1X10^6$	122	Min. Spirits
		$6.2X10^6$	154	THF
		$7.9X10^6$	167	Benzene
		$4.0X10^7$	286	CCl_4
CoMn	20[c]	$1.7X10^5$	56	Isooctane
		$1.9X10^5$	60	Benzene
		$5.2X10^5$	80	Min. Spirits
		$3.4X10^7$	320	CCl_4
Cu(CuO)	19[d]	$4.4X10^6$	121	CCl_4
		$4.3X10^8$	540	Isooctane
		$5.5X10^8$	608	Benzene
		$7.3X10^8$	668	Min. Spirits

a. Acid Composition 50% C_4, 40% C_8, 10% C_{18}

b. Acid Composition 20% C_3, 50% C_8, 15% neo C_{10}, 15% C_{18}

c. Acid Composition 20% C_3, 30% C_8, 30% neo C_{10}, 20% C_{18}

d. Acid Composition 25% C_3, 20% C_8, 25% C_{10}, 15% C_{18}, 15% C_{40}

entanglement of the longer carboxylic acid hydrocarbon chains on the surface of one particle with surface groups on other particles depends on the ability of the solvent to solvate these groups relative to the ability of surface groups to solvate one another. Further evidence to support this general mechanism of aggregation can be taken from the fact that the oil-like solvents, mineral spirits and isooctane, are the best solvents for the most complexes, i.e. the average particle size is smallest in these solutions.

In addition the extremely large particles formed by the Cu complex even in a rather good oil-like solvent such as isooctane seems consistent with the proposed aggregation mechanism when one considers just how sticky a surface coated with C_{40} acids might be toward other C_{40} coated particles. The apparent inversion of "goodness" of solvent seen for the Cu complex in Table 3 (CCl_4 giving the smallest particles) is a anomaly arising from the precipitation of most of the complex from CCl_4 solutions leaving the smaller aggregates as the average solution particles.

Specific versus non-specific aggregation has already been defined (see Figure 4.) and the data in Table 4 show specific aggregation of a Mn_3O_4 core complex in mineral spirits. Even in a good solvent like mineral spirits, aggregation was commonly encountered with the better solvents showing specific aggregation most often and the poorer solvents almost always showing non-specific aggregation.

By definition, a good solvent should yield solutions with a significant concentration of ultimate particles and small aggregates. As stated previously, the average particle size in a good

Table 4

Multiple Boundary Evidence for Specific Aggregation of a Mn_3O_4 Core Complex in Mineral Spirits

Boundary Number[a]	Sedimentation Coefficient	Molecular Weight	Number of Ultimate in the Aggregate[b]
1	120.2	$1.5X10^6$	94 (93.8)
2	83.9	$6.3X10^5$	40 (39.4)
3	41.7	$2.2X10^5$	14 (13.8)
4	33.6	$8.0X10^4$	5 (5.00)
5	29.1	$6.3X10^4$	4 (3.93)

a. see Figure 3.

b. smallest observed particle assumed to be the ultimate particles had M_w estimated to be $1.6X10^4$.

solvent is almost independent of the surface acid composition. This is reasonable since the "goodness" of the solvent would be a measure of its ability to solvate the various acid hydrocarbon tails projecting from the complexed metal oxide surface. Table 5 presents data on the particle size of some Mn_3O_4 complexes in a somewhat poorer solvent, isooctane (for comparison see Table 3 in the preceding chapter). These data indicate that the compatibility of the surface acids with the solvent is the most important factor governing the average solution particle size.

Solubility and Stability Studies. From the above discussions of particle structure (see Figure 1) and particle aggregation, it is obvious that the carboxylate composition at the surface should have a profound influence on solubility. All of the materials

Table 5

Effect of Acid Distribution on Particle Size in a Poorer Solvent

Mn_2O_3 Complexes in Iso-octane Metal/Acid	Diameter, Å	Molecular Weight
6[a]	128	$1.3X10^6$
6[b]	55	$2.4X10^5$
18[a]	76	$4.9X10^5$
18[c]	72	$4.4X10^5$
18[d]	97	$1.3X10^6$
18[e]	142	$4.8X10^6$

[a] 25% C_3, 25% C_8, 25% C_{10}, 15% C_{18}, 10% Benzoic

[b] 20% C_3, 70% neo C_{10}, 10% C_{18}

[c] 35% C_3, 35% C_8, 10% C_{10}, 15% C_{18}, 5% Benzoic

[d] 20% C_3, 40% C_8, 20% C_{18}, 20% neo C_{10}

[e] 50% C_8, 40% C_8, 10% C_{18}

prepared have shown good initial solubility in a variety of solvents including octane, iso-octane, cyclohexane, mineral spirits, mineral oil, carbon tetrachloride, benzene, and tetrahydrofuran. Most of the complexes eventually precipitate from CCl_4, benzene, and THF. The precipitation from dilute solutions is slow requiring from 24 hours to one week and is thought to reflect the time for maximum surface entanglement of separated particles. Perhaps carboxylate groups with halogenated alkyl moieties would enhance the solubility in CCl_4, while inclusion of more aromatic carboxylic acids in the surface layer might be expected to improve solubility in benzene.

The very nature of the weak ionic and H-bonding interactions holding the non-polar surface coating to the metal oxide core accounts for one of the drawbacks to the use of these materials as catalysts in reactions producing polar products. As the solvent polarity is increased, the surface groups are released from the core and precipitation of the metal oxide results. The stability of cobalt catalyst to polar solvent additives and an oxidizing agent is given in Table 6. It is clear that particle decomposition of the materials studied under mild conditions is serious and at elevated temperatures (above 100°C) and at O_2 pressures of 10 atmosphere the particle stability is even further decreased. The CoO and Mn_3O_4 soluble particles are readily destroyed by peroxides in solution and they are less stable when heated above 100° in alcohols or carboxylic acids. The cobalt particles go, in part, to $Co(OAc)_3$ when heated to 150°-200° in acetic acid.

Selected stability studies of a Mn_3O_4 core catalyst material under the more rigorous conditions are presented in Table 7. The main conclusions of the particle stability studies can be summarized as follows: 1) the core catalysts show good stability in inert solvents, e.g. cyclohexane, and in inert atmospheres (N_2) even at temperatures as high as 200°C and pressures up to 200 psi. 2) the catalyst stability is unaffected by changing the

Table 6

Catalyst Particle Stability at 25°C and Ambient Pressure With Ketone, Alcohol, and Peroxide.[a]

Sample	Additive	Observation
0.012 g CoO Catalyst 1 ml benzene	none	no ppt. or other changes after 18 hr.
"	Cyclohexanone (0.05ml)	no precipitation after 8 hr.
"	Cyclohexanol (0.05ml)	turned cloudy and some brown ppt. observed after 6 hr.
"	Cyclohexanone (0.05ml) Cyclohexanol (0.05ml)	turned cloudy and brown ppt. was observed after 5 hr.
"	t-butylhydro-peroxide (0.05ml)	darkened and ppt. appeared in 2 hr. The sample was completely precipitated in 12 hr.

[a]A similar series of studies using 0.01g of a Mn_3O_4 core catalyst in 1 ml of benzene gave the following stability order as a function of additive: no additive >>cyclohexanone >cyclohexanol >t-butyl-hydroperoxide. In 15 hrs. the complex was completely precipitated with perioxide.

atmosphere to a reducing one, e.g. H_2, CO, or a mixture of H_2 and CO, 3) the stability is decreased in an oxidizing atmosphere e.g. O_2 or O_2/N_2 mixture, 4) the catalysts are also much less stable when water, cyclohexanol, or cyclohexanone are added in small amounts and even more sensitive to the addition of carboxylic acids, and 5) exposure to peroxide causes decomposition of the metal oxides out of the core particles even at room temperature and at atmospheric pressure.

Evaluation of Soluble Metal Oxides as Precursors to Supported Catalysts

Several applications of the soluble metal oxides were described in the previous chapter. The soluble complexes had rather low catalytic

Table 7

Stability of Mn_3O_4 Core Catalyst to Various Reagents and Conditions.

Solvent & Reagent	Gas	Pressure Psig	Temp °C	Time hr.	Stability Observations and Comments
Cyclohexane/Benzene	N_2	120	195	35	no change, no ppt formed
Cyclohexane	H_2	130	178	24	no change, no ppt formed
Cyclohexane	CO	130	180	12	no change, no ppt formed
Cyclohexane	H_2/CO 1:1	135	177	24	no change, no ppt formed
Benzene	O_2/N_2	235	188	9-17	catalyst precipitates from solution
Cyclohexane/Benzene Cyclohexanone (0.2%)	N_2	195	190	8	Catalyst precipitated, solution becomes light yellow instead of normal red.
Benzene/Cyclohexane	N_2	atm.	146	12	most of catalyst ppt as a brown precipitate and solution become yellow.
Benzene/Cyclohexane	N_2	205	195	--	large amount of ppt and solution became orange.

activities in many applications but their use in preparing supported heterogenous catalysts looks quite promising. Preparation of these supported catalysts could in principle make use of the size controlling factors to achieve a particular catalytic site density or to control the size of the supported metal cluster after reduction. With this potential for surface tailoring of the support in mind, we prepared a number of catalysts. The use of the Scheme I catalysts in hydrogenations of olefins, benzene and naphthalene is described below.

Hydrogenations Over Alumina--Supported Co. 1,5-Cyclooctadiene hydrogenation was studied at 80° and 200 psi (H_2) using the $AlEt_3$-Co (Scheme I, A.) The same reaction was studied at 120° and 300 psi using the oxidized form of the catalyst (Al_2O_3-CoO). This reaction was selected because it is analogous to the hydrogenation

of olefins over supported cobalt catalysts reported in U.S. Patent 3,855,324 (2). The reactions were followed by observing the hydrogen pressure drop and terminated within 1 to 2 hrs. after no further pressure drop was observed. The solvent was hexane.

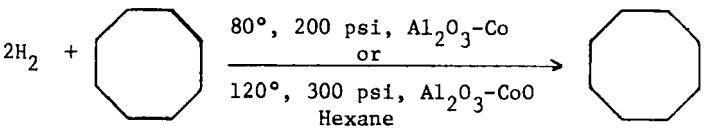

Reactions using Al_2O_3-Co at 80° were complete in about 24 hr. when 2.6 g (24.5 mmol) of diene, 4-10 ml. of hexane and 10 g of catalyst were employed. The catalyst was recycled five times without appreciable loss of activity. Hydrogenations employing the cobalt oxide catalyst Al_2O_3-CoO were much slower. When 6 g of catalyst was used with 0.9 g (8.1 mmol) of diene in 5 ml of hexane at 120°, it took 25 hrs. to achieve complete hydrogenation at 300 psi. Thus, to achieve similar hydrogenation rates, the cobalt oxide catalyst requires a temperature 40° greater than the reduced form of the catalyst.

The hydrogenation of trans, trans, cis-1,5,9-cyclododecatriene, catalyzed by the reduced Al_2O_3-Co catalyst, proceeded in the same fashion as the hydrogenations of 1,5-cyclooctadiene. The first reaction (80°, 200 psi, 15 ml hexane, 3 g triene, 10 g catalyst) gave only 37% conversion (to cyclododecane) in 48 hrs and 100% conversion in 120 hr. In each subsequent recycle reaction (same conditions except only 4 ml of hexane was used), however, the reduction was complete in 24 hr. until the fifth recycle where it took 36 hrs. to achieve complete reduction. Apparently, as was the case in 1,5-cyclooctadiene hydrogenations, the first cycle involves some reaction process at the surface to activate the catalyst. To achieve approximately equal rates, the cobalt oxide catalyst, Al_2O_3-CoO, had to be used at 120°, some 40° higher

than that of the reduced form of the catalyst, and at higher pressures (340 versus 200 psi).

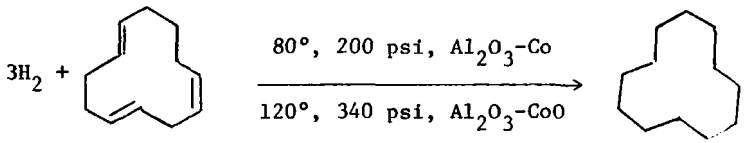

Benzene was reduced to cyclohexane over the reduced (Al_2O_3-Co) form of the supported cobalt at 80° and 200 psi of hydrogen. Remarkably, the hydrogenation of benzene occurred at a rate similar to that of the 1,5-cyclooctadiene hydrogenations. This is suprising under such mild conditions. At 80° and 200 psi, a 97% conversion to cyclohexane was achieved in 45 hrs. using 6 g of benzene and 10 g of catalyst. The catalyst used had previously been used 5 times in 1,5-cyclooctadiene hydrogenations.

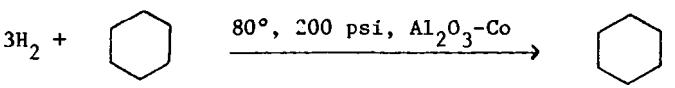

Kieselguhr-Supported Nickel Catalysts in Benzene Hydrogenations. Both the Kieselguhr-supported nickel catalyst, KG-Ni-A (reduced by hydrogen) and KG-Ni-B (reduced by $AlEt_3$), were active in promoting the hydrogenation of benzene to cyclohexane. At 80° and 200 psi hydrogen pressure the KG-Ni-B catalyst was more active. In 6 hrs., complete conversion of benzene to cyclohexane was observed using 8.8 g benzene and 5 g of catalyst. Using KG-Ni-A in an identical reaction, 77% conversion was observed in 7.5 hrs. and complete conversion was noted in 14 hrs.

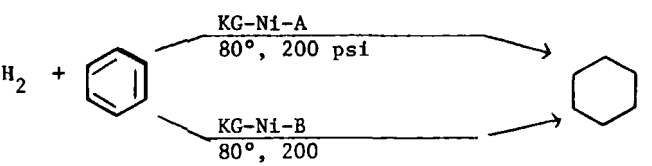

Benzene Hydrogenation Catalyzed by Al_2O_3-Fe. Benzene was readily hydrogenated to cyclohexane at 120° and 150 psi in the presence of Al_2O_3-Fe (Scheme I, C). In 14 hrs. the conversion was quantitative. It is interesting to note only traces of cyclohexane was obtained at 130° and 25-45 psi after 48 hrs. These pressure effects may signify mass transport problems. Whatever the case may be, the reductions did proceed at rather low temperatures (120°).

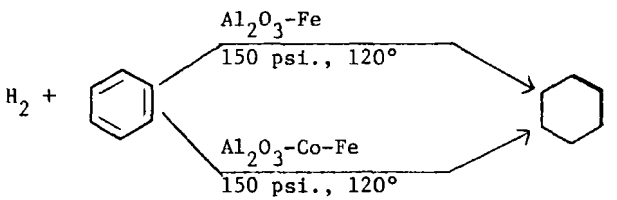

(Catalysts described in Scheme I, 7 and 8)

Benzene Hydrogenation Catalyzed by Al_2O_3-Co-Fe. Benzene was hydrogenated to cyclohexane using Al_2O_3-Co-Fe (Scheme I, D) at 120° and 150 psi of hydrogen. Using 8.8 g of benzene and 8 g of catalyst, the conversion was 94% in 15 hrs. However, hydrogenation was very slow at 25-45 psi even at 160°.

CONCLUSION

The influence of metal/acid equivalents ratio on the catalyst particle size has been demonstrated and the influence of surface carboxylate structure and solvent on particle aggregation and solubility explained in these studies. The particle stability along with the solution size and solubility of these materials are consistent with the particulate structure represented in Figure 1 and this structure, which might be described as resembling an inverted micelle, explains the rather low catalytic activity of these materials in some of the applications reported

in the previous chapter. The direct use of the soluble metal oxide materials as precursors to supported catalysts looks very good.

REFERENCES

1) A. Alkaitis and P. L. Cells, US Patent 4,163,986, Mooney Chemical Co.) 1979.

2) J. K. Mertzweiler and H. M. Tenney, US Patent 3,855,324, (Esso Research and Engineering Co.) 1971.